

A Battery-free Sensorless Thermoelectric Tag for Temperature Difference Estimation

Li Ni, Lei Che, Jiacong Qiu, and Junrui Liang

School of Information Science and Technology

ShanghaiTech University, Shanghai, China

Email: {nili2024, chelei1, qiujc, liangjr}@shanghaitech.edu.cn

Abstract—Temperature sensing is indispensable in both daily life and industrial scenarios. Thermoelectric generation, as an emerging energy harvesting technology, efficiently converts natural temperature differences into electrical energy. This study investigates a passive approach for estimating environmental temperature differences. By integrating thermoelectric generation with low-power Bluetooth communication technology, it aims to explore the correlation between Bluetooth packet transmission intervals and ambient temperature differences. To achieve this, a self-powered thermoelectric generation device has been developed and integrated with a Bluetooth module to enable low-power wireless data transmission. Experimental results demonstrate that the system can reliably send out Bluetooth signals and accurately infer temperature differences based on packet frequency. This research proposes a novel and low-cost solution for environmental monitoring. It thus exhibits broad application potential.

Index Terms—Ambient IoT, edge sensing and computing, energy management, thermoelectric energy harvesting.

I. INTRODUCTION

Energy stands as a cornerstone of modern society, underpinning economic operations, transportation systems, and daily life with its indispensable power supply. As human energy consumption continues to escalate, a significant portion of wasted energy is dissipated as low-temperature thermal gases, which in turn exacerbate climate change and global warming. For instance, in nations such as Turkey, industrial sectors are estimated to waste approximately 51% of their total heat consumption [1]. In other developed countries, such as France, it is estimated that 30% of thermal energy remains unutilized [2].

The phenomenon whereby the interface of two conductors generates a voltage under the influence of a temperature gradient is known as the Seebeck effect [3]. This effect is manifested in thermoelectric generator (TEG) components.

Thermoelectric power generation has numerous practical application scenarios and related research. In 2019, Khalil and Hassan proposed an effective method: using a TEG cooled by a natural convection radiator to enhance the waste heat recovery efficiency of chimneys, which increased the output power by approximately 64% [4]. For the road thermoelectric generator system (RTEGSS), Yuan et al. [5] compared three types of systems: pavement-subgrade, pavement-environment, and pavement-flowing water. The pavement-flowing water type RTEGSS showed the highest output voltage and a power

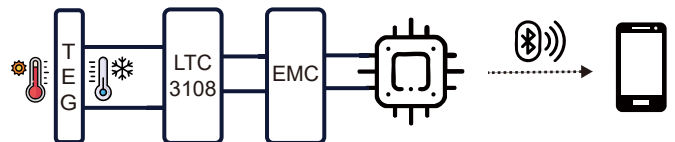


Fig. 1. System architecture.

density as high as 4.28 mW/cm^3 , outperforming systems reported in previous literature.

In research on power supply utilizing temperature differences on the surfaces of equipment such as pipes, pumps, fans, and motors, Kim et al. [6] developed a $140 \text{ mm} \times 133 \text{ mm}$ TEG, which generated 272 mW of energy from a heat pipe at $70 \text{ }^\circ\text{C}$. In addition, there is also a temperature difference between the human body and the environment. Hylan et al. [7] tested TEGs on different body parts and compared the energy generated by each part.

This paper proposes a concise battery-free and sensorless scheme for an ultra-low-cost temperature difference estimator by linking the information of temperature difference with the level of harvested power. The proposed low-cost system further enables distributed and real-time evaluation of temperature differences.

II. SYSTEM CONFIGURATION

The thermoelectric generation chips used in the experiment are made of inorganic thermoelectric materials. Specifically, these materials are BiTe-based alloys. The N-type material exhibits enhanced thermoelectric performance owing to its strong anisotropic carrier transport. The block diagram of the proposed temperature assessment system is presented in Fig. 1. The hot side of the thermoelectric generation chip is in close contact with the heat source via thermal grease. The cold side is cooled by a passive aluminum heat sink. When a temperature difference exists between the heat source and the environment, direct current (DC) is generated.

At small temperature differences, the generated energy is connected to an energy management circuit (EMC) via a boost module, enabling continuous energy accumulation. Once sufficient energy is stored to complete the transmission of Bluetooth packets, it is immediately released to transmit low-power Bluetooth broadcast packets. At this point, the receiver can receive these Bluetooth packets. Subsequently, the pro-

cesses of energy harvesting and Bluetooth packet transmission proceed cyclically.

It can be roughly inferred that with the increase of ambient temperature difference, the interval between transmitted and received broadcast packets shows obvious changes. Specifically, the larger the temperature difference, the shorter the broadcast interval. Based on this inference, an investigation is conducted to estimate the ambient temperature difference. This method uses the interval of broadcast packets. It has the characteristics of passivity, low cost, and the ability to achieve continuous real-time monitoring.

III. WORKING PRINCIPLE

A TEG consists of P-type and N-type thermoelectric materials. One end of the P-type material is connected to one end of the N-type material. This connection forms a structure, which is defined as a PN junction. For electricity generation, the two ends of this PN junction need to be placed under different temperature conditions. Under thermal excitation, the hole concentration in the P-type material at the hot end is higher than that at the cold end. Meanwhile, the electron concentration in the N-type material at the hot end is also higher than that at the cold end. This concentration difference drives holes and electrons to diffuse toward the cold region. The diffusion process of holes and electrons further induces the generation of a voltage [8].

In TEG systems, output voltage correlates directly with temperature difference. Thus, optimizing output voltage under varying temperature gradients becomes a critical research focus. In terms of energy management, simple control strategies can be adopted. These strategies allow immediate utilization of energy in thermoelectric generation systems. Such utilization does not rely on complex control systems. In specific application scenarios, such as environmental monitoring, the primary objective of thermoelectric generation may be data transmission rather than energy storage. This, in turn, influences design choices and system configurations. Consequently, exploring ways to maintain effective energy-harvesting capability under smaller temperature differences is imperative.

Taking the TEG1-199-3.5-6 TEG with dimensions of 40 mm × 40 mm as an example, experimental results demonstrate a direct proportionality between the temperature difference and the generated voltage. Experimental measurements show the following results: at a temperature difference of 10 °C, the open-circuit voltage is 0.694 V; when the temperature difference reaches approximately 70 °C, the open-circuit voltage increases to 4.92 V. The power generated under small temperature differences is usually insufficient to directly drive a micro-controller unit (MCU). Therefore, a boost circuit is required.

In energy management, the immediate utilization of energy in thermoelectric generation systems can be realized by adopting a simple control strategy. It does not rely on complex control architectures. The energy management module used in this experiment is the 3T-EM energy-aware circuit proposed by the authors' research group [9]. This circuit can successfully

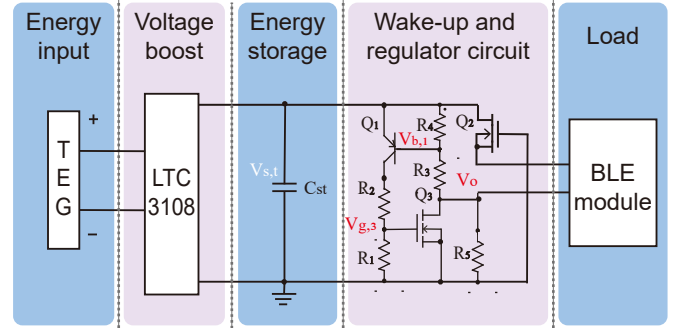


Fig. 2. Circuit topology.

start the system with an input current of only 0.4 μ A. It can also adjust the switch threshold voltage. The adjustment aims to meet customized energy requirements.

Fig. 2 shows the topology of the TEG, step-up transformer, and 3T-EM circuit. When it is in the “ON” state, Q₂ is biased in the saturation region [9]. The drain current satisfies

$$I_{ds,2} = K_{p,2} \frac{W}{L} (V_{gs,2} - V_{th,2})^2. \quad (1)$$

In the formula, $I_{ds,2}$ and $V_{gs,2}$ are the drain-source current and gate-source voltage of Q₂, respectively; $K_{p,2}$, W , L , and $V_{th,2}$ are the process constant, width, length, and threshold voltage, respectively. If a specific saturation drain current is denoted as $I_{ds0,2}$ and the corresponding gate voltage as $V_{gs0,2}$, then we can obtain

$$K_{p,2} \frac{W}{L} = \frac{I_{ds0,2}}{(V_{gs0,2} - V_{th,2})^2}. \quad (2)$$

Treating V_0 and $I_0 = I_{ds,2}$ as the load voltage and current in (1) and (2), the output voltage in the ON state can be calculated as follows

$$V_0 = -V_{th,2} - \sqrt{\frac{I_0}{I_{ds0,2}}} (V_{gs0} - V_{th,2}). \quad (3)$$

For such a depletion-mode NMOS transistor Q₃, its threshold voltage is negative. Therefore, when the load current I_0 is not very large, the output voltage can be expressed as follows

$$V_0 \approx |V_{th,2}|. \quad (4)$$

Previous studies [9] have demonstrated that this simple 3T-EM circuit can maintain a relatively stable voltage within an appropriate digital level range, while providing a maximum output current of 35 mA, which is sufficient to power most low-power MCU or system-on-chip (SoC) [10].

IV. EXPERIMENTAL EVALUATION

Tests were conducted using a TEG1-199-3.5-6 TEG. The TEG has a dimension of 40 mm × 40 mm. The experimental setup is shown in Fig. 3. To ensure better heat conduction on both sides, thermal grease is applied to the two sides of the TEG with the model number TEG1-199-3.5-6. A thermocouple was connected to sense the temperatures of the hot and cold surfaces. The TEG is then tightly attached

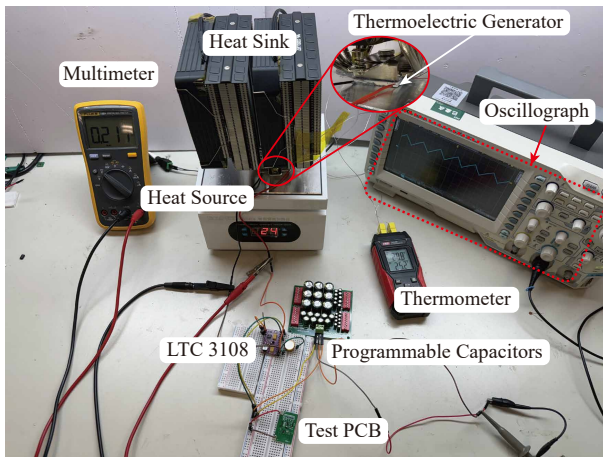


Fig. 3. Lab test setup.

to a temperature-controllable heating stage and an air-cooled heat sink. This setup enables real-time measurement of the temperature difference. The positive and negative electrodes of the TEG are connected to the LTC3108 for voltage boosting.

The LTC3108 chip is an integrated DC/DC converter specifically designed for low-power energy harvesting. It constitutes a step-up resonant oscillator through a depletion-mode N-channel MOSFET switch. It employs an external step-up transformer and a small coupling capacitor. These components function to boost input voltages. The minimum input voltage can reach 20 mV. The LTC3108 enables the module to stabilize its output voltage at approximately 5 V. This stabilization is achieved by selecting a specific mode. When the input voltage fluctuates, its built-in pulse frequency modulation (PFM) feedback circuit adjusts the switching frequency and controls the charge-discharge duration of the inductor to prevent the output voltage from exceeding 5 V due to increased input. Meanwhile, when the input voltage is relatively low, the LTC3108 accumulates energy via an external energy storage capacitor. The above process applies on the condition that the input energy is greater than or equal to the load power consumption.

The output voltage is higher than the turn-on threshold of the EMC. Thus, it is sufficient to activate the subsequent circuits. When the storage capacitor C_{st} is fully charged, the EMC starts to supply power to the load. The load then completes tasks such as Bluetooth packet transmission. With an oscilloscope, the voltage across the C_{st} capacitor can be observed in real time.

Using the test setup illustrated in Fig. 3, the following observation is obtained: within a specific temperature difference range, the charging rate of the capacitor increases with the rise of temperature difference. It is readily observed that the EMC operates in a repeated charge-discharge cycle. During the charging phase, energy is accumulated. During the discharging phase, Bluetooth packets are broadcast continuously. Here, the “packet transmission interval” is defined as the time elapsed between two Bluetooth beacon packets. Fig. 4 illustrates the

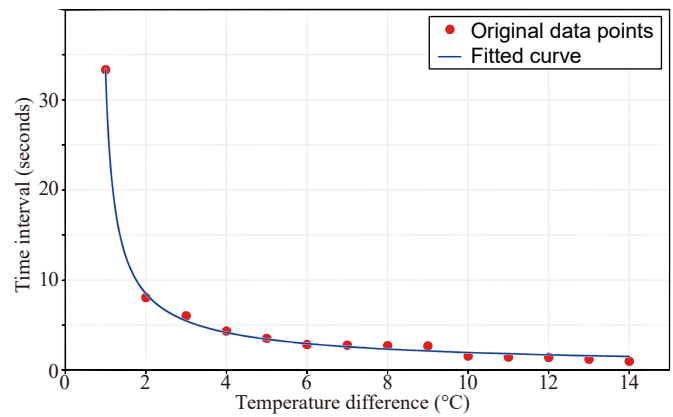


Fig. 4. Packet intervals under different temperature differences.

Bluetooth packet transmission intervals under different temperature differences. When the voltage across the thermoelectric generator does not reach the startup voltage of LTC3108 (about 35 mV), the circuit fails to start. No Bluetooth packets are transmitted in this case. When the temperature difference reaches approximately 0.7 °C, the LTC3108 starts up. At this point, the startup voltage of the LTC3108 is reached. Meanwhile, Bluetooth packets are sent out continuously.

Fig. 5 shows the voltage waveform. This waveform corresponds to buffer-release cycles. The cycles are under temperature differences of 1 °C, 2 °C, 9 °C, and 12 °C, respectively.

V. FIELD TEST

To verify the feasibility of the thermoelectric-based temperature difference estimation system in real scenarios (as a supplement to the laboratory tests in Section IV), field tests are conducted. In real environments (e.g., near industrial equipment), uncontrollable factors such as humidity and wind speed affect the heat dissipation of TEGs. To address this issue, tests were conducted indoors. The indoor room temperature is maintained at a constant 27 ± 0.5 °C using a precision air conditioner. A thermocouple with an accuracy of ± 0.1 °C is used to monitor the surface temperature of the metal heated by sunlight. This temperature monitoring enables the calculation of actual temperature differences. The above measures ensure the reliability of the TEG performance evaluation.

As shown in Fig. 6, an east-facing window is selected. The hot side of the TEG is coated with thermal grease. It is then tightly affixed to a metal surface. This metal surface is used to absorb heat from the external environment, especially sunlight. The cold side of the TEG is also coated with thermal grease. It is tightly affixed to a passive aluminum heatsink. When a temperature difference exists between the indoor and outdoor environments, the TEG-powered system transmits Bluetooth packets. These Bluetooth packets are received by an ESP32-S3 module (by Espressif Systems Ltd.). This setup enables real-time monitoring of the Bluetooth packet intervals.

To evaluate the system performance, a 24-hour monitoring of temperature differences and packet intervals is conducted.

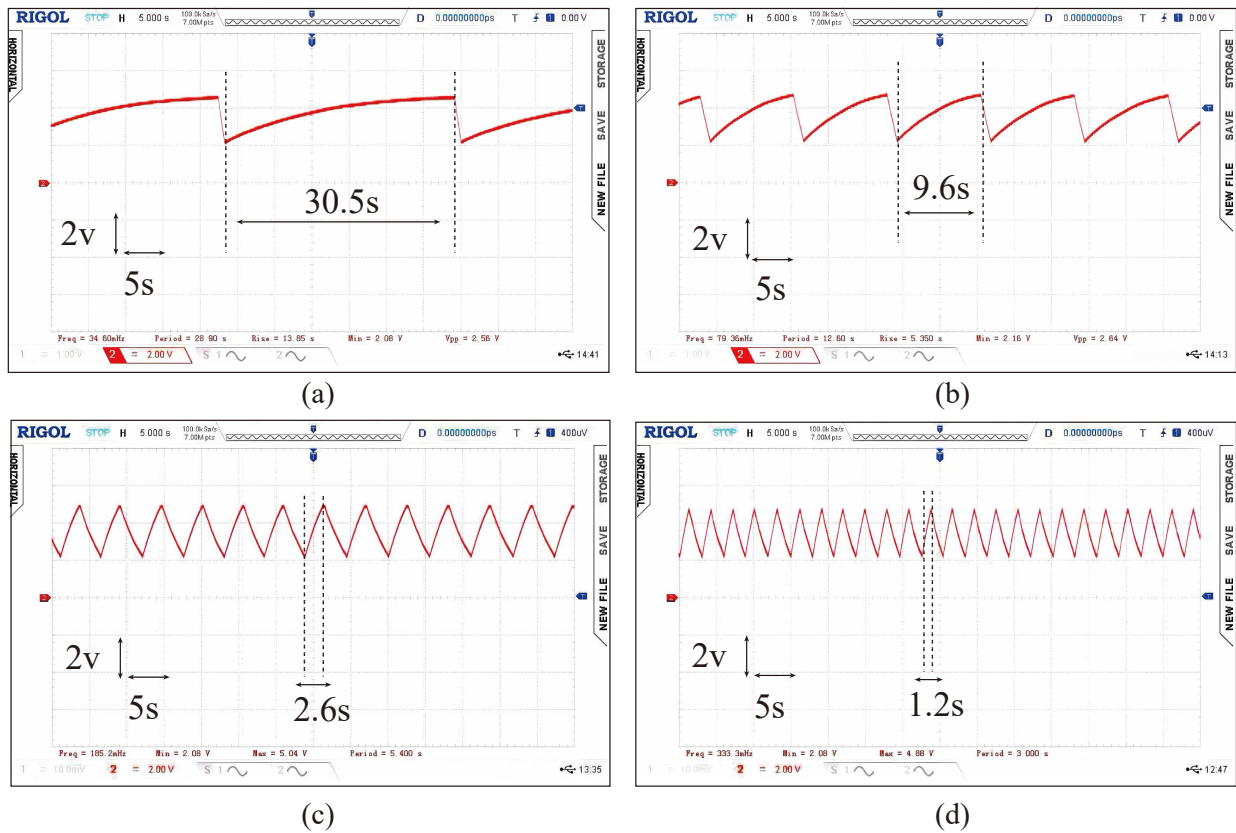


Fig. 5. Transmission intermittence under different temperature differences. (a), (b), (c), and (d) correspond to the temperature differences of 1 °C, 2 °C, 9 °C, and 12 °C, respectively.

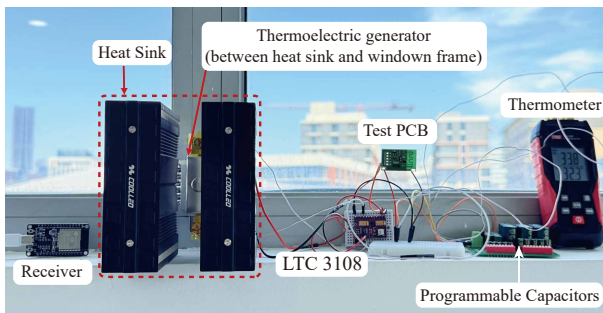


Fig. 6. Field test setup.

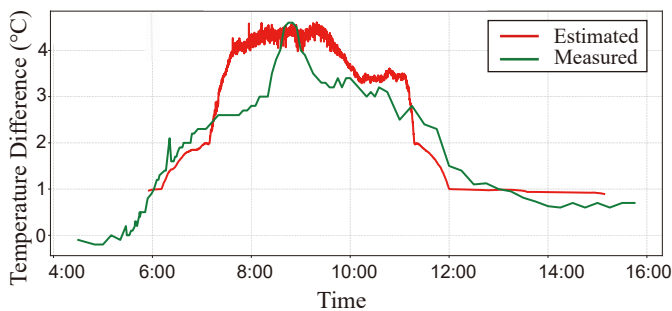


Fig. 7. Comparison of estimated and measured temperature differences.

The estimated results of temperature differences are presented in Fig. 7. Observations indicate that the accuracy in estimation decreases during periods of large temperature differences (7:30–10:00). This decline is attributed to minimal Bluetooth packet intervals and subtle time differences. During these periods, the system performs worse than that in periods with smaller temperature gradients (e.g., 6:00–7:30 and 10:00–14:00). Additionally, the system can estimate sunlight duration using Bluetooth packet intervals. When sunlight is present, the temperature difference (ΔT) exceeds 0.7 °C, and Bluetooth packet transmissions occur frequently. When there is no sunlight, Bluetooth packet intervals exceed 30 seconds or no packets are detected. In a 24-hour test, the statistically calculated sunlight duration from the system is consistent with local meteorological data. This result confirms the correlation between sunlight exposure and indoor-outdoor temperature difference.

VI. CONCLUSION

This paper introduced a battery-free and sensorless approach for temperature difference estimation. The approach integrates thermoelectric energy harvesting with Bluetooth low-energy (BLE) communication. The proposed system leveraged the correlation between BLE packet transmission intervals and ambient temperature differences. It achieves passive environmental monitoring without relying on external power sources.

REFERENCES

- [1] W.-J. Du, Q. Yin, and L. Cheng, "Experiments on novel heat recovery systems on rotary kilns," *Applied Thermal Engineering*, vol. 139, pp. 535–541, 2018.
- [2] C. Haddad, C. Périlhon, A. Danlos, M.-X. François, and G. Descombes, "Some efficient solutions to recover low and medium waste heat: competitiveness of the thermoacoustic technology," *Energy Procedia*, vol. 50, pp. 1056–1069, 2014.
- [3] N. Ashcroft, "Solid state physics," *Thomson Learning*, vol. 39, 1976.
- [4] H. Khalil and H. Hassan, "Enhancement thermoelectric generators output power from heat recovery of chimneys by using flaps," *Journal of Power Sources*, vol. 443, p. 227266, 2019.
- [5] D. Yuan, W. Jiang, A. Sha, J. Xiao, W. Wu, and T. Wang, "Technology method and functional characteristics of road thermoelectric generator system based on seebeck effect," *Applied Energy*, vol. 331, p. 120459, 2023. [Online]. Available: <https://www.sciencedirect.com/science/article/pii/S0306261922017160>
- [6] Y. J. Kim, H. M. Gu, C. S. Kim, H. Choi, G. Lee, S. Kim, K. K. Yi, S. G. Lee, and B. J. Cho, "High-performance self-powered wireless sensor node driven by a flexible thermoelectric generator," *Energy*, vol. 162, pp. 526–533, 2018. [Online]. Available: <https://www.sciencedirect.com/science/article/pii/S0360544218315962>
- [7] M. Hyland, H. Hunter, J. Liu, E. Veety, and D. Vashaee, "Wearable thermoelectric generators for human body heat harvesting," *Applied Energy*, vol. 182, pp. 518–524, 2016.
- [8] K. Uchida, S. Takahashi, K. Harii, J. Ieda, W. Koshibae, K. Ando, and et al., "Observation of the spin seebeck effect," *Nature*, vol. 455, pp. 778–781, 2008.
- [9] L. Teng, H. Wang, Y. Liu, M. Fu, and J. Liang, "A three-transistor energy management circuit for energy-harvesting-powered iot devices," *IEEE Internet of Things Journal*, vol. 11, no. 1, pp. 1301–1310, 2024.
- [10] C. Tian, Z. Chen, and J. Liang, "A battery-free and sensor-less photo-voltaic tag for real-time indoor light illuminance evaluation," in *2024 IEEE International Symposium on Circuits and Systems (ISCAS)*. IEEE, May 2024, pp. 1–5.